Supporting Information (SI)

Producing synthetic natural gas from microalgae via supercritical water gasification: A techno-economic sensitivity analysis

Brandenberger M.[a], Matzenberger J.[a,ł], Vogel F.[a], Ludwig Ch.[a,b*]

[a]Paul Scherrer Institute (PSI), General Energy Research Department (ENE-LBK),
CH-5232 Villigen PSI, Switzerland

[b]École Polytechnique Fédérale de Lausanne (EPFL), School of Architecture, Civil and Environmental Engineering (ENAC-IIE), 1015 Lausanne, Switzerland

Keywords: algae, synthetic natural gas (SNG), supercritical water gasification, sensitivity analysis, bioenergy, process economics

*Corresponding Author:

Paul Scherrer Institut

General Energy Research (ENE)

Laboratory for Bioenergy and Catalysis

CH-5232 Villigen PSI

Switzerland

Phone: +41 (0)56 310 2696

Fax: +41 (0)56 310 2199

Email: christian.ludwig@psi.ch

ł Current address:

Vienna University of Technology

Institute of Power Systems and Energy Economics

Gusshausstrasse 27-29

1040 Wien

Austria

Table of Contents

Table of Figures

Table directory

Notation

Explanations of acronyms used within text

acronyms	meaning	units
bbl	barrel	[-]
DW	dry weight	**[-]**
EROEI	energy return on energy invested	[-]
FPA	flat-panel-airlift	[-]
HT	hydrothermal	[-]
HTG	see SCWG	[-]
LCA	life cycle analysis	[-]
LHV	lower heating value	kJ g^{-1}
m^3	cubic meter at 0 ^{o}C and 0.1 MPa for gases	m^3
PBR	photobioreactor	[-]
Pc	critical pressure of water (22.06 MPa)	MPa
PWS	pressurized water scrubbing	[-]
RP	raceway ponds	[-]
SCWG	supercritical water gasification	[-]
SNG	synthetic natural gas	[-]
Tc	critical temperature of water (647.096 K)	K

TS	total solids (dry)	%
wt%	weight percent	%

Greek letters

symbol	meaning	units
$H_{u,CO}$	lower heating value of carbon monoxide	MJ m^{-3}
$H_{u,C2H6}$	lower heating value of ethane	MJ m^{-3}
H_{u,H_2}	lower heating value of hydrogen	MJ m^{-3}
H_{u,CH_4}	lower heating value of methane	MJ m^{-3}
η_{HP}	high pressure pump efficiency	%
η_{fan}	fan efficiency	%
η_{ss}	energy efficiency for the self-sufficient process	%
η_{el}	conversion efficiency of SNG to electric power	%
$\eta_{pre-heater}$	pre-heater efficiency	%
$\eta_{\mathrm{sup}er-heater}$	super-heater efficiency	%
η_{HTG}	gross energy hydrothermal gasification efficiency	%
$\eta_{process}$	overall gross thermal energy efficiency of the process	%
λ	pipe friction factor	[-]
v_{FG}^2	gas flow velocity	m s^{-1}

υ_{FG}	kinematic viscosity of flue gas	$m^2\ s^{-1}$
ϱ_{FG}	flue gas density	$kg\ m^{-3}$

Roman symbols

symbol	meaning	units
c_{loss}	fraction of water and biomass leaving the hydrothermal plant through the salt separator	%
d_{FG}	optimal pipe diameter of flue gas pipes	m
E_{PC}	effective energy required for slurry preconcentration	$MJ\ m^{-3}$
E_{FS}	effective energy required for slurry dewatering	$MJ\ m^{-3}$
E_{BF}	reference energy input belt-filter	$MJ\ m^{-3}$
E_C	reference energy input 3-chamber centrifuge	$MJ\ m^{-3}$
E_{SNG}	energy content in final product gas	TJ
E_{algae}	energy content microalgae biomass	TJ
$E_{electric}$	electric energy demand	TJ
$h_{H_2O}(T_{SCWG})$	enthalpy of water in the hot reactor effluent at 30 MPa	$kJ\ kg^{-1}$
$h_{H_2O}(T_{SP})$	enthalpy of water at salt separator temperature at 30 MPa	$kJ\ kg^{-1}$
$h_{H_2O,30\ MPa}$	enthalpy of water at 293.15 K and 30 MPa	$kJ\ kg^{-1}$
$h_{H_2O,0.1\ MPa}$	enthalpy of water at 293.15 K and 0.1 MPa	$kJ\ kg^{-1}$
$h_{wood,293K}$	enthalpy of wood at 293.15 K at 0.1 MPa °C	$kJ\ kg^{-1}$

$h_{wood}(T_{SP})$	enthalpy of wood at salt separator temperature and 0.1 MPa	kJ kg^{-1}
l_{FG}	length flue gas network	l_{FG}
Max_TS_{BF}	maximum achievable TS content for chosen belt filters	% TS
Max_TS_{C}	maximum achievable TS content for chosen centrifuge	% TS
$\dot{m}_{SCWG}$	mass flow rate of the catalytic reactor influent/effluent	kg s^{-1}
$\dot{m}_{H_2O,SP}$	water mass flow rate entering the salt separator	kg·s^{-1}
$\dot{m}_{BM,SP}$	biomass mass flow rate entering the salt separator (kg·s^{-1})	kg s^{-1}
$\dot{m}_{org,SCWG}$	mass flow of organic material entering the catalytic reactor	kg s^{-1}
$\dot{m}_{H_2O,SCWG}$	water mass flow rate entering the catalytic reactor (kg·s^{-1})	kg s^{-1}
$\dot{m}_{inorg,SP,out}$	mass flow rate of inorganic material (here N & P) leaving the SCWG plant through the salt separator	kg s^{-1}
$\dot{m}_{slag,SP,out}$	mass flow rate of organic material leaving the SCWG plant through the salt separator	kg s^{-1}
$\dot{m}_{H_2O,SP,out}$	mass flow rate of water leaving the SCWG plant through the salt separator	kg s^{-1}
$\dot{Q}_{slurry}$	harvested microalgae slurry flow rate entering belt filters	m^3 h^{-1}
$\dot{Q}_{PC}$	preconcentrated algal slurry flow rate entering centrifuges	m^3 h^{-1}
Δp_{FG}	total discharge pressure	Pa
$\dot{Q}_{pre-heater}$	heat flow rate taken up by the cold feed stream	kJ·s^{-1}
$\dot{Q}_{\mathrm{super}-heater}$	heat flow rate required by the super-heater	kJ·s^{-1}

TS_{BF}	desired TS content after preconcentration	% TS
TS_{Feed}	desired TS content in the feed for SCWG after dewatering	% TS
$\dot{V}_{FG}$	volumetric flue gas flow	$m^3 h^{-1}$
$\dot{V}_{CH_4}$	volumetric methane flow rate for the super-heater	$m^3 \cdot s^{-1}$
$\dot{V}_{H_2}$	volumetric hydrogen flow rate for the super-heater	$m^3 \cdot s^{-1}$
$\dot{V}_{CO}$	volumetric carbon monoxide flow rate for the super-heater	$m^3 \cdot s^{-1}$
$\dot{V}_{C2H6}$	volumetric ethane flow rate for the super-heater	$m^3 \cdot s^{-1}$
W_{FG}	fan power	W
W_{BF}	power consumption belt filter	W

1 Introduction

Microalgae use inorganic carbon and sunlight as carbon and energy source, both abundant natural resources. The use of microalgae would thus lower dependency on fossil fuels such as coal, petrol and natural gas. In addition, microalgae haven been put forward to capture CO_2 from industrial or atmospheric sources and thus may even qualify for carbon dioxide credits [1,2].

Microalgae are claimed to have substantially higher biomass productivities per area than terrestrial energy crops such as corn, colza, soybean, jatropha and oil palms and therefore are more suitable for the production of liquid fuels like biodiesel [3,4]. They are believed to reach productivities between 45-120 tonne of dry biomass per hectare per year and an oil yield higher than 58’700 L ha^{-1} a^{-1} based on an algal lipid content of 30% [3-5]. Moreover, microalgae do not need agricultural land and thus do not compete directly with food production compared to terrestrial energy crops who may contribute to the increase of world food prices [6,7]. Life cycle analysis (LCA) of microalgae cultivation showed that their eutrophication potential is significantly lower than for energy crops due to better runoff control of fertilizer [8]. Microalgae thus seem to be an ideal replacement for fossil fuels in the future as they are lacking many disadvantages which are commonly attributed to first and second generation biofuel technologies.

However, recent studies showed that the production of microalgae biomass requires large amounts of fertilizer, water, construction materials, electrical energy for mixing RP and PBR, water and flue gas transport as well as electrical energy for drying and harvesting of microalgae [8-10]. The production of chemical fertilizer was singled out as a main factor concerning environmental burden of algal fuels with respect to its greenhouse gas emissions, human and marine ecosystem toxicity potential as well as for the emission of acidifying substances [8,10]. In addition it has been identified that lipid extraction from microalgae consumes 90% of process energy if the lipids are obtained by dry extraction and 70% in the case of wet extraction, leading to the conclusion that such a system for purely energy generation would not yield a positive energy balance [10,11].

In order to reduce environmental impact and energy consumption from employing chemical fertilizer in microalgae production, as well as improve the economic viability of biofuels from microalgae, recycling of nutrients is a key issue. One way to achieve this is to obtain the nutrients from renewable sources like wastewater or anaerobic digestion effluent [8,12,13]. However, important additional infrastructure would be required to deliver the waste streams to the algae production facilities and may increase the risk of contamination of the microalgae cultures by bacteria or other unwanted microorganisms. In addition, there is a limited potential to recover efficiently nutrients.

Little reliable information is available concerning the economics of microalgae large scale production. Depending on the production methods, the location and the capital costs, the estimates for production costs of one kilogram of biomass can vary widely. Estimates for production costs for microalgae vary from 30 - 70 \$ kg^{-1} in closed photobioreactors [14]. The costs for microalgae biomass from raceway ponds show even larger variations and can range from 0.24 \$ kg^{-1} up to 15 \$ kg^{-1} [15]. Consequently, the estimates for one barrel of microalgae biodiesel vary in the same order of magnitude, and are estimated to be currently non-competitive with petroleum and may only by economically at a biodiesel cost of 237 \$ bbl^{-1} in combination with additional revenues, for example by selling pure proteins from algal biomass [15-17]. Clearly, future algal biomass costs need to go from the 10-100 € price range suitable for the production of pharmaceuticals, cosmetics, fine chemicals and food down to below 1 € kg^{-1} for purely energy use [18].

1.1 Principles of catalytic supercritical water gasification of biomass

Biomass conversion in supercritical water for energetic as well as chemical synthesis purposes is a well-established field of research making use of the unique properties of water above its critical point at T_c= 647.1 K and p_c=22.1 MPa [19]. Water at supercritical conditions is structurally different from ambient liquid water, as the numbers of hydrogen bonds that exist at ambient conditions in liquid water are significantly reduced. This change in number of hydrogen bonds is associated with a decrease in the dielectric constant of water to values similar of an apolar organic solvent such as THF (tetrahydrofuran), diethylether or hexane [20]. Supercritical water has therefore high miscibility for organic molecules and gases, making it thus possible to achieve tar and coke-free gasification of biomass, as tar and coke-precursors are dissolved in supercritical water. Furthermore, supercritical water supplies hydrogen atoms through the water-gas shift reaction which ultimately contributes to the production of a methane rich gas. Supercritical water is therefore not only the reaction medium but also a reactant.

2 Methodology

2.1 Technological model and performance metrics

Fig. SI 2 gives an overview of the flowsheet of the combined microalgal cultivation and catalytic hydrothermal gasification process (SunCHem process). It is assumed that the carbon dioxide is provided from a combustion source such as a coal power plant, cement plant, biogas plant with a combined heat and power plant (CHP) or a petrochemical refinery. The dry flue gas at 0 °C and 0.1 MPa is composed of 15% CO_2 and 85% N_2 [2]. The emissions of oxides of nitrogen and sulphur (NOx, SOx) and of volatile metals are not considered in the model. It is assumed that the flue gas is transported to the algal cultures after internal flue gas treatment. Flue gas is transported with axial centrifugal fans from the carbon dioxide source to the algal bioreactors by a network of welded carbon-steel pipes. Fan power W_{FG} is given by equation (2.1) with a fan efficiency η_{fan} of 85% [21]:

$$W_{FG} = \Delta p_{FG}\, \dot{V}_{FG} / \eta_{fan} \tag{2.1}$$

Where $\dot{V}_{FG}$ is the volumetric flue gas flow rate given in Table SI 1 and Δp_{FG} the total discharge pressure. Δp_{FG} is calculated with equations (2.2) - (2.4):

$$\Delta p_{FG} = (\lambda\, l_{FG}/d_{FG}) \varrho_{FG}\; v_{FG}^2/2 \tag{2.2}$$

$$\lambda = 0.3164/\sqrt[4]{Re} \tag{2.3}$$

$$Re = d_{FG}\; v_{FG}^2/\upsilon_{FG} \tag{2.4}$$

Where λ – pipe friction factor, l_{FG} – length of pipe network, d_{FG} – pipe diameter, ϱ_{FG} – flue gas density ($\varrho_{FG} = 1.123$ kg m^{-3}) [22], v_{FG}^2 – gas flow velocity and υ_{FG} – the kinematic viscosity of flue gas ($\upsilon_{FG} = 16.82$ mm^2 s^{-1}) [22]. The optimal pipe diameter d_{FG} is obtained by equation (2.5) and was calculated to be 2.57 m in the base case scenario [21]:

$$d_{FG} = 0.363\, \dot{V}_{FG}^{0.45} \varrho_{FG}^{0.13} \tag{2.5}$$

Pipe length l_{FG} is calculated based on the required footprint area for microalgae cultivation and 20% additional area taking in account additional space required for infrastructure such as buildings and roads. A circular plant layout is assumed for all three microalgae cultivation systems with the flue gas source, the SCWG plant and the dewatering units in the center as shown in Fig. SI 1. The RP/PBR are positioned around the center and are organized in modules of 100 ha size. They are connected with the control and processing units via flue gas and water pipes. The pipe network is designed according to a coarse distribution network, i.e., two circular pipes covering the cultivation area and connected with the flue gas source in the center of the facility; transport the flue gas from the source to the cultivation ponds (see Fig. SI 1). Power required for fine distribution of the flue gas is not explicitly considered in the model, but is assumed to be included in the power consumption for RP and PBR air blowers (see Table SI 1).

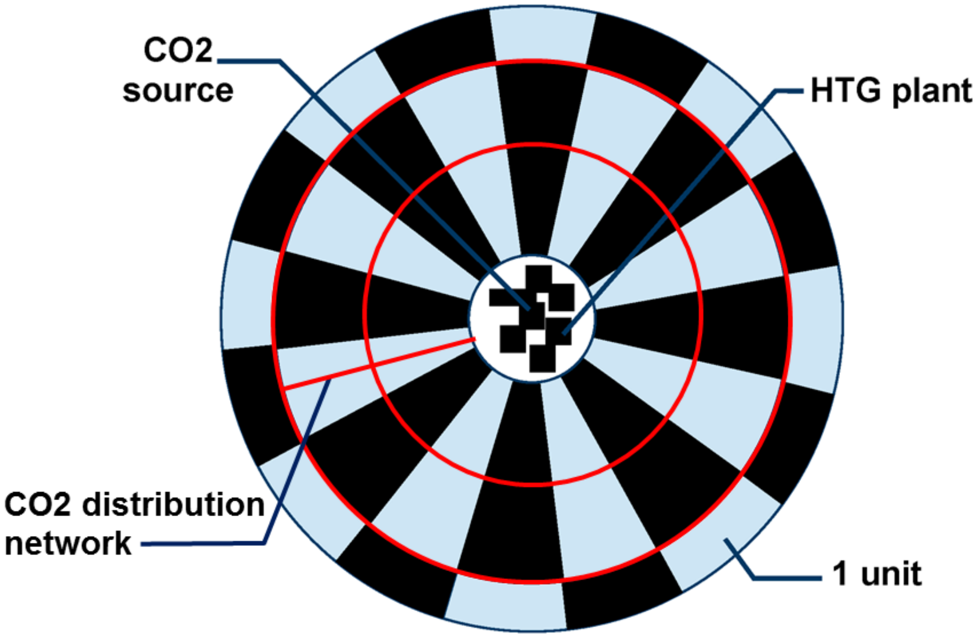

Fig. SI 1 Layout of the microalgae cultivation site with the SCWG plant in the center. Adapted from [23]

Photobioreactors (PBR) consist either of open ponds or closed PBR. Three different microalgae production scenarios are evaluated: raceway ponds (RP), tubular PBR or flat panel air lift PBR (FPA-PBR). The base parameters chosen for the three different microalgae cultivation systems based on 25% CO_2 absorption are given in Table SI 1. The assumed annual aerial surface biomass productivity (t ha^{-1} a^{-1}) determines the size of the three microalgae cultivation systems (Table SI 1). The generic algal biomass composition is assumed to be $C_1H_{1.64}O_{0.41}N_{0.13}P_{0.02}$ based on data from the ECN Phyllis database [24], with a lower heating value (LHV) of 21.904 kJ g^{-1} TS algae. The ash content of the microalgae is represented by phosphorus and nitrogen. Sulphur is not considered in the model because it is presently not considered a limited resource like phosphorus. The ash free LHV is slightly higher than the LHV of dry biomass, but both values only differ by

2.5% for the generic microalgae. C, H, O, N and P mass balances were calculated with help of equation (2.6):

$$CO_2 + 0.02PO_4^{3-} + 0.13NO_3^- + 0.725H_2O + 0.19H^+ \xrightarrow{h\nu} CH_{1.64}O_{0.41}N_{0.13}P_{0.02} + 1.393O_2 \tag{2.6}$$

The closed PBR are not actively cooled, as they are cultivated with thermophilic algal species and because we believe that actively cooled PBR's are not suitable for large-scale algae production due to the large amounts of heat, which need to be removed to keep the broth temperature between 298 K and 308 K. For a column reactor located at Merced, CA, USA, it has been calculated that 18 TJ a^{-1} respectively 5.5 TJ a^{-1} of heat need to be removed [25]. This means significant capital and operation costs associated with temperature control. Thermophiles can grow at temperatures ranging from 315 K to 348 K and therefore are suitable for closed PBR as algal broth temperature can reach between 313 K - 323 K during summer months [26-29]. For example *Chlorogleopsis sp.*, a thermophilic cyanobacteria, can grow very well at 323 K with a maximum carbon assimilation rate of 20 - 45 mg L^{-1} d^{-1}, at 200 µmol m^{-2} s^{-1}, at 5% CO_2 level and a flow rate of 0.002 L L^{-1} min^{-1} (liter gas per liter medium) [25]. The accumulation of lipids is no issue in the SunCHem process, compared with other algal biomass derived biofuels, allowing for much greater flexibility for choice of microalgae species as well as cultivation conditions.

Power consumption required to keep the microalgae in suspension and assure proper liquid/gas mass transfer during the growth phase is based on literature review and personal communications [30-32]. For FPA-PBR the power consumption lies between 100-130 W m^{-3} [33,34]. Power consumption is expressed as watt (W) per cubic meter (m^3) reactor volume. This simplification allows to compare easily the specific power input of different RP/PBR designs.

Nevertheless, the required cultivation volume depends on the reactor type and thus is a function of the volumetric algal biomass productivity specific to each RP/PBR design. Volumetric productivity (g L^{-1} d^{-1}) and biomass concentration (g L^{-1}) for the three different RP/PBR systems are based on literature review and personal communications [30-32]. Volumetric algal productivity of FPA-PBR's is presently in the range of "0.8 – 1.2 g L^{-1} d^{-1} and biomass concentration may range from 8 - 16 g L^{-1} depending on solar radiation and conditions of PBR operation" [33].Their base case values are shown in Table SI 1.

Table SI 1 Base case assumptions for three different cultivation systems based on 25% CO_2 uptake

Key parameters	**RP**	**Tubular PBR**	**FPA-PBR**
Volumetric flue gas flow rate $\dot{V}_{FG}$ (m^3 s^{-1})	75	75	75
Flue gas CO_2 vol. fraction (vol.%)	15	15	15
CO_2 up take by microalgae (%)	25	25	25
Harvesting concentration RP/PBR (g L^{-1})	0.5	3.8	8.0
Reactor volume RP/PBR (m^3)	4'492'131	181'307	309'053
Volumetric productivity (g L^{-1} d^{-1})	0.06	1.36	0.80
Surface producitivity PBR's (t ha^{-1} a^{-1})[1]	38.5	75.1	79.0
Footprint PBR for 25% CO_2 uptake (km^2)[1]	27.0	13.8	13.1
Illuminated RP/PBR area (km^2)[2]	22.5	14.5	16.2
Occupied land area/Volume ratio (m^2 m^{-3})[1]	5.0	63.5	35.4
Illuminated RP/PBR area to volume ratio (m^2 m^{-3})[2]	5.0	80.0	52.5
Harvesting ratio (%)	11.0	35.9	10.0
Power consumption RP/PBR (W m^{-3})[3]	3.7	2'500	100
Length of coarse CO_2 distribution network l (km)	20.6	14.7	14.4
Energy consumption dewatering: Belt filter E_{BF} (MJ m^{-3})[4]	0.29	0.29	0.29
Energy consumption dewatering: Centrifuge E_C (MJ m^{-3})[4]	3.60	3.60	3.60

[1] Here m^2 is used for the land area occupied by the PBR, similar for ha and km^2.

[2] Here m^2 is used for the illuminated PBR area, similar for km^2.

[3] Power required for air blowers and pumps per m^3 PBR volume for proper gas/liquid mixing and mass transfer.

[4] The power cosumption is linearized in order to take in account the change in inlet biomass concentration.

Daily production period is 10h per day with a fixed average productivity rate over the entire period. Harvesting and dewatering takes place over 24 h in order to avoid peak flows. The plant is assumed to operate 350 days per year. The assumption of continuous harvesting of algal biomass is crucial because pumping the harvested slurry consumes energy and thus pressure drop needs to be kept to a minimum. Large peak flows can cause very high energy consumption rates [35].

Microalgae are dewatered with belt filters and centrifuges to a TS content between 5 to 30 % required for SCWG of microalgae. Energy input for the belt filters and centrifuges are linearized based on algae harvesting concentration according to equations (2.7) and (2.8):

$$E_{PC} = \frac{E_{BF}}{Max\_TS_{BF}} \times TS_{BF} \tag{2.7}$$

$$E_{FS} = \frac{E_C}{Max\_TS_C} \times TS_{Feed} \tag{2.8}$$

With E_{PC} – the effective energy required to preconcentrate the algal slurry for the centrifuges with belt filers (MJ m^{-3}), E_{FS} – the effective energy input required to dewater the algal slurry to the desired feed concentration for SCWG (MJ m^{-3}), E_{BF} *and* E_c – the assumed reference energy input to preconcentrate/dewater an algal slurry with belt filters or centrifuges ($E_{BF} = 0.29$ MJ m^{-3}, $E_c = 3.6$ MJ m^{-3}) [27,36], Max_TS_{BF} and Max_TS_C – the maximum achievable TS content for the chosen belt filter or centrifuge equipment ($Max\_TS_{BF} = 9.5\%$ TS, $Max\_TS_C = 20\%$ TS), TS_{BF} and TS_{Feed} – are the desired TS content after preconcentration and algal slurry dewatering (% TS).

Power required for preconcentration W_{BF} and dewatering W_c of the algal slurry with the belt filters and centrifuges is subsequently calculated by equations (2.9) and (2.10):

$$W_{BF} = \dot{Q}_{slurry}\, E_{PC} \tag{2.9}$$

$$W_C = \dot{Q}_{PC}\, E_{FS} \tag{2.10}$$

Where $\dot{Q}_{slurry}$ – is the harvested microalgae slurry flow rate for the belt filters and $\dot{Q}_{PC}$ – the flow rate of the preconcentrated microalgae slurry entering the centrifuges. The flow rate of $\dot{Q}_{slurry}$ can be up to ~200 times higher than the flow rate $\dot{Q}_{PC}$ entering the centrifuges. Such a preconcentration step is necessary as the dry solid content of algal biomass in the harvested algal broth is usually below 1% TS and therefore the algal broth needs to be preconcentrated before dewatering the slurry to the desired final solid content by costly and energy intensive centrifugation. Belt filters, however, are only suitable for harvesting relatively large microalgae species such as *C. proboscideum* or *S.platensis*. A collection of different types of belt filters and centrifuges, including their energy consumption and relative harvesting cost, has been published by Grima *et al.* and Mohn [27,36]. State of the art dewatering technology achieves today up to >99% biomass recovery [37]. Therefore, with a microalgae optimized for dewatering, this value is plausible as any assumed significant loss of biomass in mass cultivation of microalgae would be unreasonable with respect to the longterm viability of such a process. Algal harvest efficiency is thus assumed here to be 100%.

The permeate from the filtration and centrifugation step, containing a large fraction of the nutrients, is recycled and reused for algal cultivation without further treatment. The remaining microalgae slurry is stored in tanks to ensure 24 hours continuous operation of the SCWG plant. Storage capacity is designed to last for a maximum of 4 days at 293.15 K. We expect 4 days to be a reasonable maximal storage time to minimize material losses due to anaerobic digestion of algal biomass, which requires significant longer retention times and temperatures [38].

The algal slurry is pumped with a high pressure pump to the desired pressure of 30 MPa. Power input for the high pressure pump W_{HP} is given by equation (2.11):

$$W_{HP} = (h_{H_2O,30\,MPa} - h_{H_2O,0.1\,MPa})\,(\dot{m}_{H_2O,SP} + \dot{m}_{BM,SP})/\eta_{HP} \tag{2.11}$$

With $h_{H_2O,30\,MPa}$ and $h_{H_2O,0.1\,MPa}$ – the enthalpy of water at 293.15 K and 30 MPa, respectively at 0.1 MPa (kJ kg^{-1}), $\dot{m}_{H_2O,SP}$ and $\dot{m}_{BM,SP}$ – the mass flow rates of water and biomass being pumped (kg s^{-1}), η_{HP} – is the mechanical pump efficiency of the high pressure pump. The same enthalpy has been assumed for the biomass and water mass flow rates, due to the lack of information of the physical properties of algal biomass at 30 MPa and 293.15 K. By attributing the same enthalpy to the biomass as for the water, a conservative approach is being made, because the algal biomass can be considered to be a fully incompressible solid.

Heat from the reactor effluent is used to preheat the algal slurry to a temperature of 643.15 K. Water evaporation is avoided by heating the slurry up under high pressure, i.e. above the critical pressure of water at 22.1 MPa.

Heat recovery from the hot reactor effluent to the pre-heater is calculated with equation (2.12):

$$\dot{Q}_{pre-heater} = \dot{m}_{SCWG}\left(h_{H_2O}(T_{SCWG}) - h_{H_2O,30\,MPa}\right)\eta_{pre-heater} \tag{2.12}$$

$\dot{Q}_{pre-heater}$ is the heat flow rate transferred from the hot reactor effluent to the cold feed stream in the pre-heater (kJ s^{-1}), $\dot{m}_{SCWG}$ – the mass flow rate of the catalytic reactor influent/effluent (kg s^{-1}), $h_{H_2O}(T_{SCWG})$ – the enthalpy of water in the hot reactor effluent (kJ kg^{-1}), $h_{H_2O,30\,MPa}$ – the enthalpy of water at 293.15 K (kJ kg^{-1}), which is the assumed inlet temperature of the algal biomass slurry. $\eta_{pre-heater}$ – the pre-heater efficiency calculated with AspenPlus® (Aspentech 2006, USA). All the enthalpies are at a pressure of 30 MPa. The enthalpies of the product gases are neglected.

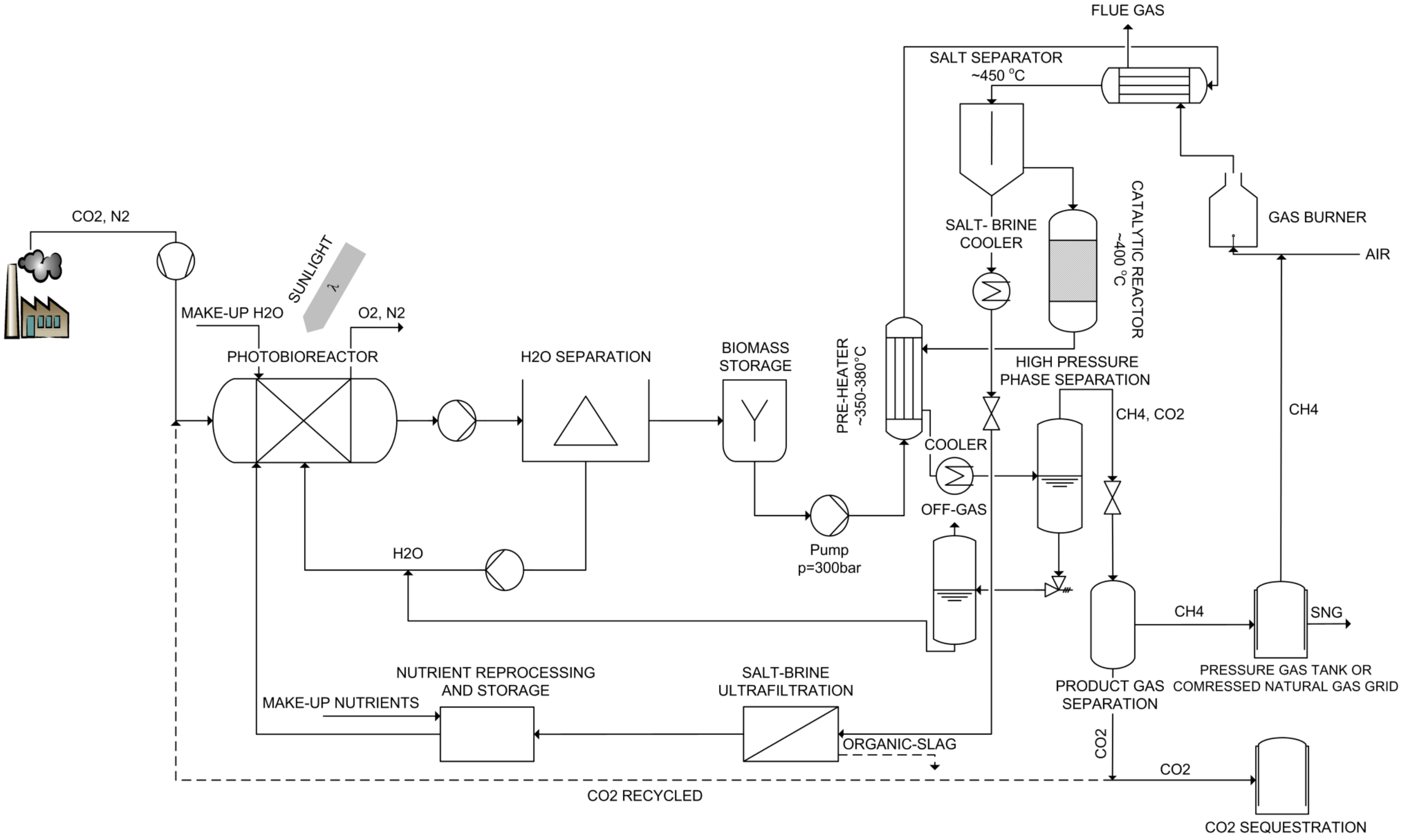

Fig. SI 2 Flowchart of the combined microalgae cultivation and catalytic supercritical water gasification process (SunCHem process)

In a next step the slurry is superheated in the salt separator to the supercritical state. At these conditions, the nutrients precipitate because the fluid exhibits a very low solubility for salts [39-41] The salt separator (SP) consists of a reverse flow gravity separator, where the salt brine leaves at the bottom ($\dot{m}_{inorg,SP,out} + \dot{m}_{slag,SP,out} + \dot{m}_{H_2O,SP,out}$) and the organic phase at the top of the SP ($\dot{m}_{org,SCWG}$, see Fig. SI 2). The salt brine is cooled and treated with an ultrafiltration unit so that it can be recycled to the PBR. The organic material leaving the SP with the salt brine is removed in the ultrafiltration unit and can be recycled back to the hydrothermal gasification process. It may be possible to directly feed the nutrient concentrate to the PBR. To be on the safe side however, salt separator effluent conditioning by ultrafiltration was assumed necessary. Table SI 2 gives the key parameters used to design the ultrafiltration unit [42,43].

Table SI 2 Ultrafiltraton unit

Key parameters ultrafiltration unit	Value
Operating pressure (kPa)	525
Energy consumption (MJ m^{-3})	10.8
Rate of flux (m^3 m^{-2} d^{-1})	0.61
Capital cost membrane (€ m^{-2})	842
Membrane replacement costs (€ m^{-2} a^{-1})	105

The salt separator is the hottest part in the SCWG process, which consequently requires that a fraction of the product gas (methane), has to be burned to supply enough heat to drive the SCWG. The salt separator is heated by the hot flue gas leaving the burner. The net overall process efficiency of the SCWG plant is expected to reach 60–70%, defined as the lower heating value of the net methane produced to the lower heating value of the TS content fed to the SCWG plant. The main parameters of the SCWG plant are shown in Table SI 3.

Table SI 3 Summary of the main parameters for the SCWG part

Key parameters SCWG	**Value**
Feed concentration: TS_{Feed} (% TS)	20
$Feed_{SCWG}$ (kg s^{-1})	14.3
$\dot{m}_{BM,SP}$ (kg s^{-1})	2.9
$\dot{m}_{H2O,SP}$ (kg s^{-1})	11.4
$\dot{m}_{inorg,SP,out}$ (kg s^{-1})	0.3
$\dot{m}_{slag,SP,out}$ (kg s^{-1})	0.3
$\dot{m}_{H2O,SP,out}$ (kg s^{-1})	1.1
$\dot{m}_{SCWG}$ (kg s^{-1})	12.6
c_{loss} (%)	10.0
$\eta_{pre\text{-}heater}$ (%)	72
$\eta_{super\text{-}heater}$ (%)	89.3
$T_{pre\text{-}heater}$ (K)	643
T_{SP}(K)	723
T_{SCWG} (K)	703
Pressure (MPa)	30

Equation (2.13) calculates the heat required by the super-heater (or salt separator) $\dot{Q}_{super-heater}$ in kg s^{-1}:

$$\dot{Q}_{super-heater} = \frac{\dot{m}_{H_2O,SP}\left(h_{H_2O}(T_{SP}) - h_{H_2O,30\ MPa}\right) + \dot{m}_{BM,SP}\left(h_{wood}(T_{SP}) - h_{wood,293\ K}\right) - \dot{Q}_{pre-heater}}{\eta_{super-heater}} \qquad (2.13)$$

Where $\dot{m}_{H_2O,SP}$ – the water mass flow rate entering the SP (kg s^{-1}), $\dot{m}_{BM,SP}$ – the biomass mass flow rate entering the SP (kg s^{-1}), $h_{H_2O}(T_{SP})$ – the enthalpy of water at SP temperature and 30 MPa (kJ kg^{-1}), $h_{H_2O,30\ MPa}$ – the enthalpy of water at 293.15 K and 30 MPa (kJ kg^{-1}), $\dot{Q}_{pre-heater}$ – the heat flow transferred in the pre-heater (kJ s^{-1}), $h_{wood}(T_{SP})$ and $h_{wood,293\ K}$ are the enthalpies of wood at 293 K and at salt separator temperature. Both enthalpies are at a pressure of 0.1 MPa. The enthalpies of wood were used in place of the enthalpies of algal biomass, which are not precisely known. Indeed, the change of enthalpy for biological material at different reaction conditions compared to the change of enthalpy for water is small. Thus, it is a reasonable assumption to assume the same enthalpy for algal biomass as for wood. For example the apparent heat capacity for shrimps (w_{H2O} = 80%) is 3.63 J g^{-1} K^{-1} whereas the value used in this work is 1.2 J g^{-1} K^{-1} for dry wood [44,45]. $\eta_{super-heater}$ – the super-heater heat transfer efficiency calculated with

AspenPlus® (Aspentech 2006, USA) and defined as the heat flow transferred from the hot flue gases from the process burner to the fluid inside the salt separator (super-heater).

The remaining fluid stream containing the organic fraction and water is gasified and converted to methane and CO_2, with small amounts of H_2, CO, C_2H_6 in the catalytic reactor.

The mass flow rate $\dot{m}_{SCWG}$ (kg s^{-1}) entering the catalytic reactor is expressed by equation (2.14):

$$\dot{m}_{SCWG} = \dot{m}_{org,SCWG} + \dot{m}_{H_2O,SCWG} = \left(\dot{m}_{BM,SP} + \dot{m}_{H_2O,SP}\right)(1 - c_{loss}) - \dot{m}_{inorg,SP,out} \qquad (2.14)$$

Where $\dot{m}_{org,SCWG}$ is the mass flow rate of organic material after the SP in kgs^{-1}, $\dot{m}_{H_2O,SCWG}$ – the water mass flow rate after the SP (kg s^{-1}), $\dot{m}_{H_2O,SP}$ – the water mass flow rate entering the SP (kg s^{-1}), $\dot{m}_{BM,SP}$ – the biomass mass flow rate entering the SP (kg s^{-1}), c_{loss} – the fraction of water and biomass which leaves the SCWG plant through the SP and $\dot{m}_{inorg,SP,out}$ – the mass flow rate of inorganic material (here N and P) leaving the SCWG plant through the SP (kg s^{-1}). The organic material leaving the SCWG plant through the SP, shown as organic-slag in Fig. SI 2, is not further considered in the model. Of course, it would be technically feasible to recycle the organic slag to the SCWG unit. Therefore, this part of the organic feed is lost and thus the model underestimates the biomass conversion efficiency. Indeed, by setting c_{loss} to zero, biomass conversion efficiency >70% could be reached. However, a conservative value for $c_{loss} = 10\%$ was assumed because experimental work with model organic compounds in a continuous laboratory scale plant showed that $c_{loss} \leq 10$ % [46].

A heat loss leading to a reactor exit temperature T_{SCWG} 20 K lower than the salt separator temperature T_{SP} was assumed. The gas composition leaving the isothermal catalytic reactor was calculated with AspenPlus® (Aspentech 2006, USA) using Gibbs free energy minimization and based on the elemental composition of the algal biomass. A variant of the Peng-Robinson equation of state was used (called PR-BM in AspenPlus®) The AspenPlus® model assumes that the nutrients N and P are separated in the salt separator, i.e., before gasification as NH_3 and PO_4^{3-}. In summary, the elemental composition of the biomass changes in the SP as indicated by equation (2.15):

$$CH_{1.64}O_{0.41}N_{0.13}P_{0.02} \rightarrow CH_{1.25}O_{0.41} + 0.13NH_3 + 0.002H_3PO_4 + 0.03H_2O \tag{2.15}$$

Equation (2.16) gives the equilibrium composition, calculated by AspenPlus®, of the final product gas after the hydrothermal catalytic reactor as a function of temperature “T”, pressure “p” and biomass concentration “c” in the feed ($\alpha, \beta, \gamma, \delta, \varepsilon, \epsilon = f(T, p, c)$):

$$CH_{1.25}O_{0.41(s)} + \alpha H_2O_{(l)} \rightarrow \beta CH_{4(g)} + \gamma CO_{2(g)} + \delta H_{2(g)} + \varepsilon CO_{(g)} + \epsilon C_2H_{6(g)} \tag{2.16}$$

The methane flow rate to the gas burner is calculated with equation (2.17):

$$\dot{V}_{CH_4} = \frac{\dot{Q}_{super-heater} - \left(\dot{V}_{H_2}\, H_{u,H_2} + \dot{V}_{CO}\, H_{u,co} + \dot{V}_{C2H6}\, H_{u,C2H6}\right)}{H_{u,CH_4}} \tag{2.17}$$

$\dot{V}_{CH_4}$ is the volumetric methane flow rate for the super-heater in m^3 s^{-1}, $\dot{V}_{H_2}, \dot{V}_{CO}, \dot{V}_{C2H6}$ – the volumetric hydrogen, carbon monoxide and ethane flow rate for the super-heater (m^3 s^{-1}), $\dot{Q}_{super-heater}$ – the required heat flow rate to be provided to the super-heater to reach the desired temperature in the SP (kJ s^{-1}) and $H_{u,CH_4}, H_{u,H_2}, H_{u,co}, H_{u,C2H6}$ – the lower heating values of methane, hydrogen, carbon monoxide and ethane (kJ m^{-3}). These components (CH_4, H_2, CO and C_2H_6) are internally separated from the product gas and valorized in the gas burner for heat supply in the SP (see also Fig. SI 2).

The gross energy efficiency η_{SCWG} (%) of converting algal biomass into methane is expressed by equation (2.18):

$$\eta_{SCWG} = \frac{E_{SNG}}{E_{algae}} 100 \tag{2.18}$$

Where E_{SNG} is the energy contained in the final product gas and E_{algae} the energy contained in the feedstock (algae) both variables being expressed in TJ a^{-1}. E_{algae} is calculated based on the lower heating value of microalgae on a dry matter basis (see above).

In case of a totally self-sufficient process, electricity required for the microalgae cultivation and for the SCWG plant auxiliaries (e.g. pumps) needs to be produced by converting part of the SNG into electricity in a modern combined cycle gas turbine (CCGT). For state of the art CCGT a power production efficiency of $\eta_{el} = 55\%$ can be assumed [47]. The energy efficiency for the self-sufficient SunCHem process is expressed through the energy return on energy invested (EROEI) performance indicator. The EROEI is defined according to equation (2.19):

$$EROEI = \frac{Usable\ Acquired\ Energy}{Energy\ Expended} = \frac{E_{SNG}}{\frac{E_{required}}{\eta_{el}}} \tag{2.19}$$

Where $E_{required}$ is the sum of all power requirements for the SunCHem process (see "*Table 1 Energy return on energy invested (EROEI) for RP, tubular PBR and FPA-PBR*" in the main article) for a detailed list of process units taken in consideration.

By cooling the catalytic reactor effluent, the water is condensed out and the remaining CO_2 is separated by pressurized water scrubbing (PWS) from the methane in a concentrated form (enrichment factor of 800-1000 compared to the inlet CO_2 concentration), which may be fed to an underground store [48]. Alternatively, the CO_2 can be used for microalgae cultivation.

Capital cost for PWS is calculated based on 713 € m^3 h^{-1} throughput of treated raw gas and power consumption is assumed to be 0.54 MJ m^{-3} raw gas [49]. The loss of methane gas in the PWS unit is considered to be 0 %, although PWS units usually have a methane loss between 1-2 %, depending on the operation conditions. However, the waste gas stream from the PWS separation unit can be used to provide the required process heat for the SCWG plant.

CO_2 sequestration or internal recycling was not taken into account although shown in Fig. SI 2.

2.2 Economic model and performance metrics

The investment costs of the algal biomass cultivation systems are estimated through rating and costing of the major process equipment and are based on literature data and personal communications from manufacturers [12,15,32,43,50,51]. The material costs to build one FPA-PBR photosynthetic unit are 25% of the total investment costs of a fully equipped FPA-PBR microalgae production facility and “one hectare of a fully equipped FPA-PBR costs about 1.5 M€” [52]. Cost estimations for the SCWG gasification plant were based on Gasafi *et al.* [53], adjusted with a scaling factor of 0.6 based on the throughput of the HTG plant. Nutrient costs are taken into account in order to replace some of the nitrogen and phosphorus lost during the recycling process. A recycling efficiency for nutrients of 25% is assumed in the base case. However, we think that this value represents a rather low recycling value because mostly only organic material is supposed to be removed in the ultrafiltration unit. Furthermore, it has been shown, that with a salt separator consisting of a reverse flow gravity separator, salts could be recovered with efficiencies between 80 -

97% [39-41] For estimating direct and indirect costs and other expenditures, ratio factors were assumed based on delivered equipment costs, which include the most basic features of a microalgae cultivation stage, i.e., the material to build the raceway ponds or PBR, the paddle wheels, the air blowers and pumps to keep the algal broth in suspension or the nutrients pumps, but not the axial air blowers to transport the flue gas and the pumps to transport the alga forth and back to the dewatering units. These were accounted for separately. Ratio factors for flue gas transport, RP/PBR and biomass storage were based on Grima *et al*. [27], for all the other components ratio factors from Gasafi *et al.* were used [53]. Depreciation is calculated with a period of 15 years. Insurance costs are assumed to be 0.5% of the yearly depreciation. Similar assumptions were made for tax cost and interest rate for debt capital which amount to 20%, and 6%, respectively, of the yearly depreciation (based on 100% debt capital).

A summary of the assumptions made to calculate the overall economic performance is given in Table SI 4. The numbers of employees required per 100 ha are based on Norsker et al. [54] and Weissman et al. [55]. The catalyst used in our experimental work and published in several articles is a commercial catalyst from BASF with 2 weight percent Ruthenium on an activated carbon support [48]. A detailed overview of obtained results for the construction and production costs of the SunCHem process at different scenarios is given in Table SI 5.

Table SI 4 Economic assumptions

Parameter	Unit	Value	
Delivered equipment costs RP/PBR (includes cultivation units, air blowers, paddle wheels and pumps)			
Raceway ponds	€ ha^{-1}	20'000	-
Tubular PBR	€ ha^{-1}	460'000	-
FPA-PBR	€ ha^{-1}	460'000	-
Investment costs		**RP/PBR**	**SCWG plant and other infrastructure**
Installation cost	%	40	39
Instrumentation and control	%	15	13
Piping	%	40	31
Electrical	%	10	10
Buildings	%	20	39
Yard improvements	%	10	10
Service facilities	%	20	55
Engineering and supervision	%	30	32
Land	%	0	6
Running costs			
Maintenance (% from investment costs)	%	4	4
Contractor's fee (% from investment costs)	%	5	10
Contingency (% from investment costs)	%	6	15
Depreciation	a	15	15
Insurance (% from depreciation)	%	0.5	0.5
Debt service, 100% equity (% from depreciation)	%	6	6
Tax (% from depreciation)	%	20	20
General plant overheads (% from maintenance and labor costs)	%	55	55
Raw materials			
Culture medium phosphorus	€ t^{-1}	1000	-
Culture medium nitrogen	€ t^{-1}	800	-
Catalyst (lifetime 1 year)	€ t^{-1}		400'000
Water	€ m^{-3}	1	1
Utilities			
Power	€ GJ^{-1}	30.6	30.6
Labor			
Workers	Persons per 100 ha	7	-
Salary	€ h^{-1}	20	20
Operational hours	h a^{-1}	8'400	8400
Supervision	%	20	20
Payroll charges	%	25	25

Table SI 5 Overview construction and production costs for the SunCHem process: Base, optimistic and very optimistic scenarios

	Base case			Optimistic scenario			Very optimistic scenario		
Parameter/Process unit	**RP + SCWG**	**Tubular PBR + SCWG**	**FPA-PBR + SCWG**	**RP + SCWG**	**Tubular PBR + SCWG**	**FPA-PBR + SCWG**	**RP + SCWG**	**Tubular PBR + SCWG**	**FPA-PBR + SCWG**
Construction costs culture system (€ ha^{-1})	64'602	1'485'846	1'485'846	35'531	817'215	817'215	6'460	148'585	148'585
Construction costs culture system incl. harvesting & storage (€ ha^{-1})	416'911	1'605'414	1'564'837	265'531	912'712	887'675	210'615	244'119	222'882
Construction costs SCWG (€ ha^{-1})	14'360	28'018	29'454	18'722	36'529	38'402	22'234	43'382	45'607
Construction costs SunCHem process (€ ha^{-1})	442'814	1'655'955	1'617'970	301'376	982'651	961'200	255'508	331'712	314'967
Labour costs (€ ha^{-1} a^{-1})	27'342	27'342	27'342	27'342	27'342	27'342	27'342	27'342	27'342
Total production costs (€ ha^{-1} a^{-1})	97'931	477'622	276'014	74'854	269'872	175'069	62'153	98'245	71'303
Production costs of algal biomass (€ kg^{-1} TS)	2.42	6.24	3.38	1.21	2.30	1.39	0.75	0.59	0.39
Production costs SNG (€ GJ^{-1})	194	484	266	90	167	103	53	43	30
Production costs (in %)									
Algae culture and harvesting	**%**	**%**	**%**	**%**	**%**	**%**	**%**	**%**	**%**
Flue gas transport	1.7	0.5	0.9	2.6	1.0	1.6	3.5	3.0	4.1
Photobioreactors/Raceway ponds	10.5	26.9	46.8	8.9	26.8	41.4	0.9	11.7	15.8
Dewatering	26.4	1.3	1.2	20.3	1.4	1.1	19.8	3.3	2.4
Power for air blowers/Paddle wheels	3.0	44.4	5.5	1.8	36.6	4.0	0.6	25.8	2.5
Water circulation pumps	1.5	0.3	0.4	1.7	0.4	0.6	2.1	1.1	1.3
Biomass storage	0.03	0.01	0.02	0.05	0.02	0.04	0.06	0.08	0.11
Catalytic SCWG	**%**	**%**	**%**	**%**	**%**	**%**	**%**	**%**	**%**
HP Pumps	0.20	0.08	0.15	0.20	0.11	0.17	0.11	0.13	0.19
SCWG	1.9	0.8	1.4	3.4	1.9	3.0	5.0	6.1	8.7
Gas separation	1.5	0.6	1.1	2.5	1.4	2.2	3.2	3.9	5.6
Ultrafiltration	0.05	0.02	0.03	0.07	0.04	0.06	0.09	0.11	0.15
Overheads/Labour	**%**	**%**	**%**	**%**	**%**	**%**	**%**	**%**	**%**
Maintenance	16.3	12.5	21.1	14.4	13.0	19.6	14.3	11.6	14.9
Plant overheads	9.0	6.9	11.6	7.9	7.2	10.8	7.9	6.4	8.2
Labour	18.0	3.7	6.4	23.3	6.5	10.0	27.4	17.2	23.2
Overheads labour	9.9	2.0	3.5	12.8	3.6	5.5	15.1	9.4	12.8
	100.00	100.00	100.00	100.00	100.00	100.00	100.00	100.00	100.00
Production costs incl. labour (in %)									
Algae culture and harvesting	43.1	73.4	54.7	35.4	66.3	48.7	27.0	45.0	26.2
Catalytic SCWG	3.7	1.5	2.7	6.2	3.4	5.4	8.4	10.3	14.6
Overheads/Labour	53.2	25.1	42.6	58.4	30.3	45.8	64.6	44.7	59.1
Overheads/Labour, algae culture and harvesting	96.3	98.5	97.3	93.8	96.6	94.6	91.6	89.7	85.4
Only labour costs	27.9	5.7	9.9	36.1	10.1	15.5	42.4	26.6	36.0
Capital cost distribution (in %)									
Construction costs biomass production	14.6	89.7	91.8	11.8	83.2	85.0	2.5	44.8	47.2
Construction costs incl. Harvesting and storage	94.2	96.9	96.7	88.1	92.9	92.4	82.4	73.6	70.8
Catalytic SCWG and gas cleaning	5.8	3.1	3.3	11.9	7.1	7.6	17.6	26.4	29.2

2.3 Sensitivity analysis

As stated before the analyzed process refers to a hypothetical system, it is therefore plausible to assume a capital cost estimation accuracy with an error of < 25% in all estimates, although we used sound assumptions and tried to minimize the proportion of arbitrary choice to design a realistic SNG process [56]. In order to overcome the inherent uncertainties of a hypothetical system, however, a sensitivity analysis is performed covering a wide range of values. The parameters studied in this work and the ranges of variation are given in Table SI 6 and Table SI 7.

Table SI 6 Selected parameters for the energy sensitivity analysis. Variation of parameters is given in percentage (%) with respect to the values in the base cases

Range of variation	**Parameter**	**RP + SCWG**	**FPA-PBR + SCWG**
-50% - +50%	Energy required by air blowers: Gas-liquid mass transfer and mixing of the algal culture ($J\ s^{-1}\ m^{-3}$).	1.86 - 5.58	50 - 150
-50% - +50%	Dewatering energy: Energy required by belt filters to treat 1 m^3 of algal broth per dry weight percent ($kJ\ m^{-3}\ \%\ TS^{-1}$).	15.12 - 45.36	15.12 - 45.37
-50% - +50%	Dewatering energy: Energy required by centrifuges to treat 1 m^3 of algal broth per dry weigtht percent ($kJ\ m^{-3}\ \%\ TS^{-1}$).	90 - 270	91 - 270
-50% - +300%	Harvesting concentration: Concentration at which microalgae are harvested ($g\ L^{-1}$).	0.25 - 2	4 - 32
-25% - +100%	Biomass productivity: Productivity of biomass on a fixed land area per year ($t\ ha^{-1}\ a^{-1}$).	29 - 77	60 - 158
-75% - +50%	SCWG feed concentration: Weight fraction of dry algal biomass in liquid slurry entering the hydrothermal process (% TS).	10 - 30	10 - 30
-40% - +360%	CO_2 up take by microalgae: Fraction of emitted flue gas CO_2 fixed by algal biomass (%).	10% - 90%	10% - 90%

Table SI 7 Selected parameters for the economic sensitivity analysis. Variation of parameters is given in percentage (%) with respect to the values in the base cases

Range of variation	**Parameter**	**RP + SCWG**	**FPA-PBR + SCWG**
-50% - +50%	Energy required by air blowers: Gas-liquid mass transfer and mixing of the algal culture (J s^{-1} m^{-3}).	1.86 - 5.58	50 - 150
-50% - +50%	Dewatering energy: Energy required by belt filters to treat 1 m^3 of algal broth per dry weight percent (kJ m^{-3} % TS^{-1}).	15.12 - 45.36	15.12 - 45.36
-50% - +50%	Dewatering energy: Energy required by centrifuges to treat 1 m^3 of algal broth per dry weigtht percent (kJ m^{-3} % TS^{-1}).	90 - 270	91 - 270
-50% - +300%	Harvesting concentration: Concentration at which microalgae are harvested (g L^{-1}).	0.25 - 2	4 - 32
-25% - +100%	Biomass productivity: Productivity of biomass on a fixed land area per year (t ha^{-1} a^{-1}).	29 - 77	60 - 158
-75% - +50%	SCWG feed concentration: Weight fraction of dry algal biomass in liquid slurry entering the hydrothermal process (% TS).	10 - 30	10 - 30
-100% - +100%	Nutrient price: Costs of 1 kg of fresh nutrients (€ kg^{-1}). Here only for $NaNO_3$ and KH_2PO_4.	1 - 1.6 | 0 - 2	0 - 1.6 | 0 - 2
-100% - +100%	CO_2 credits: Additional income per tonne of CO_2 replaced by burning BIO-SNG instead of fossil CH_4 (€ t^{-1}).	0 - 36	0 - 36
-75% - +75%	Electricity cost: Cost of one power unit (€ GJ^{-1}).	7.6 - 53.5	7.6 - 53.5
-40% - +360%	CO_2 up take by microalgae: Fraction of emitted flue gas CO_2 fixed by algal biomass (%).	10% - 90%	10% - 90%
-90% - +50%	Construction costs: Compounded costs for one hectare land covered with RP/PBR (only material), including circulation pumps (€ ha^{-1})	2'000 - 30'000	46'000 - 690'000

Aknowledgment

The authors gratefully acknowledge P. Ripplinger and U. Schmid-Staiger from Subitec for providing data. M. Janssen, M. Schubert, M. Rüdisüli and A. Haiduc for valuable discussions and C. Gattiker for providing Fig. SI 1. This project was made possible through financial support from the Velux Foundation, Zürich (project Nr. 405), Competence Center Energy and Mobility (CCEM) and swisselectric research in the frame of the SunCHem project.

References

[1] Gouveia L. Microalgae as a Feedstock for Biofuels. SpringerBriefs in Microbiology. Springer Berlin Heidelberg; 2011.

[2] Kadam KL. Microalgae Production from Power Plant Flue Gas: Environmental Implications on a Life Cycle Basis. Golden CO: National Renewable Energy Laboratory; 2001 June. 55 p. Report No.: NREL/TP-510-29417.

[3] Chisti Y. Biodiesel from microalgae. Biotechnol Adv. 2007 May;25(3):294–06.

[4] Brennan L, Owende P. Biofuels from microalgae–A review of technologies for production, processing, and extractions of biofuels and co-products. Renew Sust Energy Rev. 2010 Feb;14(2):557–77.

[5] Pulz O. Evaluation of GreenFuel's 3D Matrix Algae Growth Engineering Scale Unit, APS Red Hawk Power Plant, AZ June - July, 2007. Red Hawk AZ: IGV Institut für Getreideverarbeitung GmbH; 2007 September. 14 p. Sponsored by GreenFuel Technologies Corporation.

[6] Johansson D, Azar C. A scenario based analysis of land competition between food and bioenergy production in the US. Clim Change. 2007 June;82(3):267–91.

[7] Godfray HCJ, Crute IR, Haddad L, Lawrence D, Muir JF, Nisbett N, et al. The future of the global food system. Philos Trans R Soc Lond B Biol Sci. 2010 Sep;365(1554):2769–77.

[8] Clarens AF, Resurreccion EP, White MA, Colosi LM. Environmental Life Cycle Comparison of Algae to Other Bioenergy Feedstocks. Environ Sci Technol. 2010 Mar;44(5):1813–19.

[9] Stephens E, Ross IL, King Z, Mussgnug JH, Kruse O, Posten C, et al. An economic and technical evaluation of microalgal biofuels. Nat Biotech. 2010 Feb;28(2):126–28.

[10] Lardon L, Hélias A, Sialve B, Steyer JP, Bernard O. Life-Cycle Assessment of Biodiesel Production from Microalgae. Environ Sci Technol. 2009 Sep;43(17):6475–81.

[11] Razon LF, Tan RR. Net energy analysis of the production of biodiesel and biogas from the microalgae: Haematococcus pluvialis and Nannochloropsis. Appl Energy. 2011 October;88(10):3507–14.

[12] Borowitzka MA. Micro-algal biotechnology. Borowitzka MA, Borowitzka LJ, editors. Cambridge GB: Cambridge University Press; 1988.

[13] Van Iersel S, Gamba L, Rossi A, Alberici S, Dehue B, Van de Staaij J, et al. ALGAE-BASED BIOFUELS: A Review of Challenges and Opportunities for Developing Countries. Rome IT: Food and Agriculture Organization of the United Nations (FAO); 2009 May. 49 p. Report No.: 33.

[14] Sheehan J, Dunahay T, Benemann J, Roessler P. A Look Back at the U.S. Department of Energy's Aquatic Species Program-Biodiesel from Algae: Close-out Report. Golden CO: National Renewable Energy Laboratory; 1998 July. 328 p. Report No.: NREL/TP-580-24190.

[15] van Beilen JB. Why microalgal biofuels won't save the internal combustion machine. Biofuel Bioprod Bior. 2010;4(1):41–52.

[16] Carlsson AS, Van Beilen JB, Möller R, Clayton D. Micro- and macro- algae: Utility for industrial applications. Bowles D, editor. EPOBIO. CPL Press; 2007. EPOBIO is supported by the European Commission under the Sixth RTD Framework Programme Specific Support Action SSPE-CT-2005-022681 together with the United States Department of Agriculture.

[17] Williams PJlB, Laurens LML. Microalgae as biodiesel & biomass feedstocks: Review & analysis of the biochemistry, energetics & economics. Energy Environ Sci. 2010;3(5):554–90.

[18] Ripplinger P. Algen: Kritische Auseinandersetzung, Möglichkeiten, Wirtschaftlichkeit; 2009. [cited 2011 Jul 17]. Available from: http://www.carmen-ev.de/dt/portrait/symposien/symp_09/vortraege/Ripplinger.pdf.

[19] Peterson AA, Vontobel P, Vogel F, Tester JW. In Situ Visualization of the Performance of a Supercritical Water Salt Separator Using Neutron Radiography. J Supercrit Fluids. 2008;43:490–99.

[20] Akiya N, Savage PE. Roles of Water for Chemical Reactions in High-Temperature Water. Chem Rev. 2002 Aug;102(8):2725–50.

[21] Peters MS, Timmerhaus KD, West RE. Plant Design and Economics for Chemical Engineers. 5th ed. Glandt ED, Klein MT, Edgar TF, editors. McGraw-Hill; 2003.

[22] Pipe flow calculations.com [Internet]; www.pipeflowcalculations.com; c2011 [cited 2011 Jul 23]. Available from: http://www.pipeflowcalculations.com/tables/flue-gas.php.

[23] Gattiker C. Assessment of production and hydrothermal conversion of microalgae to synthetic natural gas for transportation [master thesis]. Lausanne (VD): École Polytechnique Fédérale de Lausanne (EPFL); 2009.

[24] ECN Phyllis - the composition of biomass and waste [Internet]; Petten (NL). Energy Research Centre of the Netherlands; c2011 [cited 2011 Aug 18]. Available from: http://www.ecn.nl/phyllis/single.html.

[25] Béchet Q, Shilton A, Fringer OB, Muñoz R, Guieysse B. Mechanistic Modeling of Broth Temperature in Outdoor Photobioreactors. Environ Sci Technol. 2010 Mar;44(6):2197–03.

[26] Mascarelli AL. Algae: fuel of the future? Environ Sci Technol. 2009 Sep;43(19):7160–61.

[27] Grima EM, Fernandez FGA, Medina AR. Downstream Processing of Cell-Mass and Products. In: Richmond A, editor. Handbook of Microalgal Culture. Blackwell Publishing Ltd; 2007. p. 215–252.

[28] Ono E, Cuello JL. Carbon Dioxide Mitigation using Thermophilic Cyanobacteria. Biosyst Eng. 2007 Jan;96(1):129–34.

[29] Tredici M, Materassi R. From open ponds to vertical alveolar panels: the Italian experience in the development of reactors for the mass cultivation of phototrophic microorganisms. J Appl Phycol. 1992 Sep;4(3):221–31.

[30] Jorquera O, Kiperstok A, Sales EA, Embiruçu M, Ghirardi ML. Comparative energy life-cycle analyses of microalgal biomass production in open ponds and photobioreactors. Bioresour Technol. 2010 Feb;101(4):1406–13.

[31] Sierra E, Acién FG, Fernández JM, Garcia JL, González C, Molina E. Characterization of a flat plate photobioreactor for the production of microalgae. Chem Eng J. 2008 May;138(1-3):136–47.

[32] Grima EM, Belarbi EH, Fernandez FGA, Medina AR, Chisti Y. Recovery of microalgal biomass and metabolites: process options and economics. Biotechnol Adv. 2003 Jan;20(7-8):491–15.

[33] Dr. Ulrike Schmid-Staiger from Frauenhofer IGB, emailed personal communication; 2009 October 5.

[34] unknown reviewer, emailed personal communication; 2011 May 26.

[35] Murphy CF, Allen DT. Energy-Water Nexus for Mass Cultivation of Algae. Environ Sci Technol. 2011 Jun;45(13):5861–68.

[36] Mohn FH. Harvesting of micro-algal biomass. In: Borowitzka MA, Borowitzka LJ, editors. Micro-algal biotechnology. Cambridge GB: Cambridge University Press; 1988. p. 395–14.

[37] Evodos - Separation Excellence. Today [Internet]; www.evodos.eu; c2011 [cited 2011 Dez 29]. Available from: http://www.evodos.eu/market-specific-solutions/totally-dewatering-algae.html.

[38] Sialve B, Bernet N, Bernard O. Anaerobic digestion of microalgae as a necessary step to make microalgal biodiesel sustainable. Biotechnol Adv. 2009;27(4):409–16.

[39] Schubert M, Aubert J, Müller JB, Vogel F. Continuous salt precipitation and separation from supercritical water. Part 3: Interesting effects in processing type 2 salt mixtures. J Supercrit Fluids. 2012 Jan;61(0):44–54.

[40] Schubert M, Regler JW, Vogel F. Continuous salt precipitation and separation from supercritical water. Part 1: Type 1 salts. J Supercrit Fluids. 2010;52:99–12.

[41] Schubert M, Regler JW, Vogel F. Continuous salt precipitation and separation from supercritical water. Part 2: Type 2 salts and mixtures of two salts. J Supercrit Fluids. 2010;52:113–24.

[42] Tchobanoglous G, Burton FL, Stensel HD. Wastewater engineering: treatment and reuse. 4th ed. Tata Mc Graw-Hill Publishing Company Limited; 2003.

[43] Cheryan M. Ultrafiltration Handbook. Technomic Publishing Company, Inc.; 1986.

[44] Simpson W, TenWolde A. Physical Properties and Moisture Relations of Wood; 1999. p. 3-1-3-24. In: Wood handbook–Wood as an engineering material. Forest Products Laboratory; Report No.: GTR-FPL-113. Sponsored by the U.S. Department of Agriculture.

[45] Karunakar B, Mishra SK, Bandyopadhyay S. Specific heat and thermal conductivity of shrimp meat. J Food Eng. 1998 Aug;37(3):345–51.

[46] Schubert M. Catalytic hydrothermal gasification of biomass - salt recovery and continuous gasification of glycerol solutions [dissertation]. Zurich (ZH): ETH Zurich, No. 19039; 2010.

[47] Polyzakis AL, Koroneos C, Xydis G. Optimum gas turbine cycle for combined cycle power plant. Energ Convers Manage. 2008 Apr;49(4):551–63.

[48] Stucki S, Vogel F, Ludwig C, Haiduc AG, Brandenberger M. Catalytic gasification of algae in supercritical water for biofuel production and carbon capture. Energy Environ Sci. 2009;2(5):535–41.

[49] Weidner E, Urban W, Girod K, Lohmann H. Technologie und Kosten der Biogasaufbereitung und Einspeisung in das Erdgasnetz. Ergebnisse der Markterhebung 2007-2008. Fraunhofer-Institut; 2008. Report No.: 4.15. Contract No.: 01LS05039. Sponsored by Bundesministerium für Bildung und Forschung (BMBF).

[50] Tapie P, Bernard A. Microalgae production: Technical and economic evaluations. Biotechnol Bioeng. 1988;32(7):873–85.

[51] Benemann RJ, Oswald JW. Systems and economic analysis of microalgae ponds for conversion of CO2 to biomass. Dept. of Civil Engineering, University of Berkeley; 1996 March. Grant No.: DE-FG22-93PC93204. Sponsored by the U.S. Department of Energy.

[52] Dr. P Ripplinger, Subitec GmbH, Germany, emailed personal communication; 2010 January 19.

[53] Gasafi E, Reinecke MY, Kruse A, Schebek L. Economic analysis of sewage sludge gasification in supercritical water for hydrogen production. Biomass Bioenergy. 2008 Dec;32(12):1085–96.

[54] Norsker NH, Barbosa MJ, Vermuë MH, Wijffels RH. Microalgal production - A close look at the economics. Biotechnol Adv. 2011;29(1):Suppl Design Basis:S11.

[55] Weissman JC, Goebel RP. Design and Analysis of Microalgal Open Pond Systems for the Purpose of Producing Fuels. Golden CO: Solar Energy Research Institute; 1987 April. 214 p. Report No.: SERI/STR-231-2840.

[56] Biegler LT, Grossmann IE, Westerberg AW. Systematic methods of chemical process design. Prentice-Hall international series in the physical and chemical engineering sciences. Prentice Hall; 1997.